

Accepted Manuscript

This document is the Accepted Manuscript version of a Published Work that appeared in final form in *Environmental Science and Technology*, copyright © American Chemical Society after peer review and technical editing by the publisher.

To access the final edited and published work see
<http://dx.doi.org/10.1021/acs.est.9b07821>

Foppe Smedes, Jaromír Sobotka, Tatsiana P. Rusina, Pavla Fialová, Pernilla Carlsson, Radovan Kopp, and Branislav Vrana. 2020, 54, 13, 7942–7951.
Unraveling the Relationship between the Concentrations of Hydrophobic Organic Contaminants in Freshwater Fish of Different Trophic Levels and Water Using Passive Sampling.
Environmental Science & Technology.

It is recommended to use the published version for citation.

1 Unraveling the relationship between concentrations of
2 hydrophobic organic contaminants in freshwater fish of
3 different trophic levels and water using passive sampling

4
5 *Foppe Smedes*^{1, *}, *Jaromír Sobotka*¹, *Tatsiana P Rusina*¹ *Pavla Fialová*¹, *Pernilla*
6 *Carlsson*^{1,2}, *Radovan Kopp*³ and *Branislav Vrana*¹

7 ¹ Masaryk University, Faculty of Science, Centre RECETOX, Kamenice 753/5, 625 00 Brno, Czech
8 Republic

9 ² Norwegian Institute for Water Research (NIVA), Fram Centre, Hjalmar Johansen gate 14, 9007 Tromsø,
10 Norway

11 ³ Mendel University in Brno, Faculty of AgriSciences, Department of Zoology, Fisheries, Hydrobiology and
12 Apiculture (FA), Zemědělská 1, 61300 Brno, Czech Republic

13

* Corresponding author:

Foppe Smedes

foppe.smedes@recetox.muni.cz

Masaryk University, Faculty of Science, Centre RECETOX

Kamenice 753/5, pavilon A29

625 00 Brno

Czech Republic

14 **Abstract**

15 Concentrations of hydrophobic organic compounds (HOC) in aquatic biota are used for
16 compliance, as well as time and spatial trend monitoring in the aqueous environment (EU WFD,
17 OSPAR). Due to trophic magnification in the food chain, thermodynamic levels of HOC, e.g. PCB,
18 DDT and BDE, in higher trophic level (TL) organisms are expected to be strongly elevated above
19 those in water. This work compares lipid-based concentrations at equilibrium with the water phase
20 derived from aqueous passive sampling ($C_{L\rightleftharpoons\text{water}}$), with lipid-based concentrations in fillet and liver
21 of fish (C_L) at different TL for three water bodies in the Czech Republic and Slovakia. HOC's C_L in
22 fish were near $C_{L\rightleftharpoons\text{water}}$, only after trophic magnification up to TL=4. For fish at lower TL, C_L
23 progressively decreased relative to $C_{L\rightleftharpoons\text{water}}$ as HOC's K_{ow} increased above 10^6 . The C_L decreasing
24 towards the bottom of the food chain suggests non-equilibrium for primary producers (algae), which
25 is in agreement with modeling passive HOC uptake by algae. Because trophic magnification and
26 resulting C_L in fish exhibit large natural variability, $C_{L\rightleftharpoons\text{water}}$ is a viable alternative for monitoring of
27 HOC using fish, showing a twofold lower confidence range while requiring less samples.

28

29

30 **Introduction**

31 Many chemical substances can leach into the environment as a result of their use in products, direct
32 application or waste discharge. Their presence may harm ecosystems, depending on amount,
33 distribution, degradation rate and toxicity. Hence, production and usage of several of these
34 compounds are restricted or banned. To assess the effectiveness of measures to reduce pollution, trend
35 and compliance monitoring is performed in water, sediment or biota.¹⁻³ Apart from assessing potential
36 impact on organisms, concentrations of hydrophobic organic compounds (HOC, see Supporting
37 information S1 for acronym explanation)) in biota are often used for monitoring the aquatic
38 environment because bioaccumulation processes result in HOC concentrations in biota being much
39 higher than in water and thus are analytically more feasible to measure. However, HOC levels in biota
40 depend on various biological confounding factors, such as the lipid content of organisms, their sex,
41 age, feeding habits, food availability, migration behavior and seasonality. Furthermore,
42 biomagnification assessment of HOC requires consideration of organisms' trophic level (TL)^{4,5}, in
43 combination with correction for other non-controllable factors such as lipid content. In monitoring
44 programs, the influence of biological confounding factors is reduced by sampling pre-selected species
45 of a certain age, size and sex.^{5,6} However, despite the attempts to minimize the sampling variability,
46 the inherent biological variability complicates the monitoring of HOC for compliance as well as for
47 spatial and temporal trend assessment.^{7,8}

48 Aqueous passive sampling (PS) has a great potential as an alternative to biota sampling^{9,10} and the
49 estimated freely dissolved concentration is proportional to the chemical activity, representing bio-
50 availability of the HOC.¹¹ In contrast to aquatic organisms or whole water, partitioning passive
51 samplers (e.g. based on silicone or low-density polyethylene polymer) provide "samples" from the
52 environment with HOC concentrated in a matrix of well-characterized and constant properties. HOC
53 accumulation in passive samplers (PS) is driven by the gradient in chemical activity between the
54 aqueous phase and the PS until thermodynamic equilibrium is attained. The resulting equilibrium
55 concentration in the PS (C_p) has been suggested as a kind of "Chemometer",¹² as C_p in PS equilibrated
56 with environmental media, e.g. water, sediment, and also biota tissue, allows direct comparison of

57 HOC's thermodynamic level between these media, but also between different ecosystems on a global
 58 scale. However, to eliminate differences between the various polymers that can be used, C_p obtained
 59 for various environmental media can conveniently be converted to a lipid-based concentration
 60 ($C_{L\rightleftharpoons\text{media}}$) through multiplication by HOC's lipid-polymer partition coefficient (K_{LP})¹² allowing a
 61 simple comparison of HOC levels across media.^{10,13-15} This includes fish tissue for which $C_{L\rightleftharpoons\text{tissue}}$ can
 62 be obtained by equilibrium passive sampling (EPS), performed by placing a PS in fish fillet. EPS
 63 provides data equivalent to C_L in fish fillet measured after classical solvent extraction.^{16,17} Note that
 64 $C_{L\rightleftharpoons\text{water}}$ or $C_{L\rightleftharpoons\text{sediment}}$ should not be understood as a direct prediction of internal HOC concentration in
 65 aquatic organisms, but rather as the thermodynamic HOC level in the monitored habitat the fish is
 66 exposed to. The thermodynamic level of persistent HOC, expressed as C_L , is often observed to
 67 increase from primary producers, through primary consumers towards predators, and a linear
 68 relationship with the trophic level (TL) can be fit to those observations:⁵

$$\log C_L^{\text{TL}(x)} = \log C_L^{\text{TL}(y)} + \{\text{TL}(x) - \text{TL}(y)\} \log TMF \quad (1)$$

69 where a $C_L^{\text{TL}(x)}$ is HOC's lipid-based concentration in a fish species of $\text{TL}(x)=x$, the intercept $C_L^{\text{TL}(y)}$ is
 70 e.g. the C_L for a primary producer ($y=1$) or other selected TL, and TMF is the lipid-based trophic
 71 magnification factor, i.e. the factor by which C_L increases for each unit of TL. The general assumption
 72 is that trophic magnification progressively elevates C_L above $C_{L\rightleftharpoons\text{water}}$ and $C_{L\rightleftharpoons\text{sediment}}$ in the habitat.
 73 However, recent literature reports C_L for PCB in fishes of TL up to 4 being lower than $C_{L\rightleftharpoons\text{sediment}}$.^{12,13,18}
 74 To unravel this phenomenon, an HOC's C_L or $C_{L\rightleftharpoons\text{tissue}}$ can be compared to $C_{L\rightleftharpoons\text{water}}$ in order to position
 75 the thermodynamic HOC level in fishes at various TL against that in the water phase. Hereto various
 76 fish species are sampled comprising the available range in TL in three selected water bodies in the
 77 Czech Republic and Slovakia having different levels of contamination. In the fish fillet and liver,
 78 HOC's C_L are determined by solvent extraction and $C_{L\rightleftharpoons\text{tissue}}$ by EPS. To estimate $C_{L\rightleftharpoons\text{water}}$, PS is applied
 79 in water including conventional¹⁹ and dynamic passive sampling.²⁰ Subsequently, bioaccumulation
 80 and biomagnification at various TL are evaluated in relation to HOC's thermodynamic level in the
 81 water phase obtained by PS and the observations compared with the current understanding of
 82 biomagnification. The outcome is rationalized through modeling the equilibration rate of the passive

83 HOC uptake by phytoplankton (bottom of aquatic food chains). Finally, implications in relation to
84 chemical biota monitoring practices⁵ are discussed and compared with passive sampling.

85

86 **Experimental**

87 **Target HOC** included in this research were penta- and hexa-chlorobenzene (PeCB and HCB),
88 polychlorinated biphenyl congeners (PCB 28, 52, 101, 118, 138, 153 and 180), DDx (2,4'-DDE, 4,4'-
89 DDE, 2,4'-DDD, 4,4'-DDD, 2,4'-DDT 4,4'-DDT) and 6 brominated diphenyl ether congeners (BDE
90 28, 47, 99, 100, 153 and 154).

91 **Fish sampling and aqueous phase PS. Site A** is a fishpond (S2-1) where five adult fish species
92 at various trophic levels were sampled: i.e. grass carp, common carp, ide, bronze bream and wels
93 catfish (see S3 for Latin names and acronyms, feeding pattern, numbers, length and weight ranges).
94 Nine adult fish of similar size were collected for each species (S3). Swan and duck mussels were
95 sampled from the fishpond as a baseline reference for primary consumers (TL=2) for estimation of
96 TL of sampled fishes. Because of the large range in size, duck mussels were divided in two size
97 classes (S5). During a six months period prior to fish sampling, stationary PS was applied in the water
98 outlet of the pond and dynamic PS,²⁰ using forced water flow to enhance HOC's sampler uptake,
99 from the bank of the pond²¹ (S4-1). At Site A, two types of silicone were applied for sampling: SSP
100 (SSP-M823, 0.0125 cm thickness, Shielding Solutions Limited, UK) and Altesil (0.05 cm thickness,
101 www.altecweb.com). PS preparation is briefly described in S7-1 and for all sites passive sampling
102 was performed following available guidelines.¹⁹ **Site B** is located in the PCB contaminated river
103 Laborec (S2-2), downstream of a former PCB production plant²² in eastern Slovakia. Adult fish from
104 the following species were collected by electro-fishing: asp, perch, European chub, common bleak,
105 roach, crucian carp, common nase, bronze bream and common barbel (S3). Only three individual
106 mussels (swollen river mussel) could be sampled, which were combined to one sample (S5). Altesil
107 PS were deployed stationary at three locations (S2) during two consecutive periods between March
108 and August 2017 (S4-2). **Site C** is the mountain river Bečva, which flows in the northeastern part of
109 the Czech Republic (S2-3). In two electro-fishing events, adult fish of only European chub, common

110 nase and common barbel, could be sampled (S3). No mussels were available from site C. At two
111 selected positions (S2-3), Altesil PS were deployed from the right- and left-hand riverbank for six
112 months (S4-3). All fish and passive samplers were stored at -20°C until processing.

113 **Fish sample processing.** Body lengths and weights were recorded for each individual fish and
114 the ranges are presented in S3. If the total fish weight for a single species was more than 10 kg,
115 individuals were divided into two groups by separating odd and even numbers after ordering them by
116 body weight. If the group consisted of an odd number of fish the last was divided between both
117 groups. Asp, caught at site B, was divided into three size groups due to very large individual size
118 differences. Following the protocol in S6, fillet and liver or hepatopancreas (both referred to as liver),
119 were pooled per fish group. For small fishes, e.g. roach and common bleak, and the fishes from Site C,
120 only fillets were collected (S4). Fillets of each fish group were cut into cubes of ~1.5 cm size and
121 manually mixed. A 300 g portion of fish cubes was homogenized with a kitchen blender. The water
122 content was determined based on the weight loss after drying 5 g homogenate overnight at 105°C
123 (S12). Another 5 g of homogenate was freeze-dried and used for the determination of $\delta^{15}\text{N}$ as the
124 fractional difference of the isotope ratio ($^{15}\text{N}/^{14}\text{N}$) in the sample and nitrogen in air (‰) by the
125 method described in S8-1. For chemical analysis of HOCs internal standards were added to 10-60 g
126 of homogenate followed by solvent extraction with a cyclohexane/isopropanol/water mixture²³ (S8-
127 2). Utilizing a portion of the extract (20-50%), the lipid content was determined as the weight
128 remaining after solvent evaporation and drying at 105 °C until constant weight (S12). Another portion
129 of the extract (20-50%) was concentrated to 1-2 mL hexane and subjected to a destructive cleanup by
130 elution over sulfuric acid loaded silica (S8-5) followed by concentration to 100 μL and instrumental
131 analysis (S8-6). Liver tissue of the corresponding fish species followed the same procedure as for
132 fillets. The chemical analysis provided HOC concentrations in fillet and liver, which were expressed
133 on lipid-basis (C_L).

134 EPS was applied by equilibrating >1 kg of fillet cubes or >0.2 kg liver tissue pieces and SSP
135 passive samplers (S7-1) as described in S-8.3.¹⁷. After extraction of the SSP (S8-4), cleanup (S8-5),
136 and instrumental analysis (S8-6), the equilibrium HOC concentrations in the SSP were converted to

137 lipid-basis ($C_{L\rightleftharpoons\text{tissue}}$) by multiplying with the lipid (triolein/fish oil)–polymer partition coefficient
 138 (K_{LP}) for SSP. For neutral lipids, these K_{LP} are not lipid specific and are available for PCB, PeCB,
 139 HCB and DDx.^{24,25} The K_{LP} for BDE were estimated as the ratio of C_L and C_P equilibrated with fillet
 140 by EPS for samples from site B and C (highest BDE levels) as described for SSP in S9-1.

141 **Aqueous passive sampling.** For HOC with a $\log K_{ow} > 6$, equilibrium is not readily attained by
 142 PS deployed in surface waters²¹ and in such cases the concentration in the sampler polymer at
 143 equilibrium ($C_{P\rightleftharpoons\text{water}}$) is calculated using a first order uptake kinetics model adapted from Smedes
 144 and Booij:¹⁹

$$C_{P\rightleftharpoons\text{water}} = \frac{N_t/m}{1 - \exp\left(-\frac{B t}{M^{0.47} K_{PW} m}\right)} \quad (2)$$

145 where N_t is the HOC mass (ng) accumulated after time t (d) in a sampler of mass m (kg). K_{PW} (L kg⁻
 146 ¹) is the HOC's polymer–water partition coefficient, M is the HOC's molar mass (g mol⁻¹), and B is
 147 a deployment-specific proportionality constant representing the local exposure conditions and
 148 sampler geometry. This B is estimated from measured retained fractions of performance reference
 149 compounds (PRC) that were dosed to the sampler prior to exposure. PRC fractions retained after
 150 exposure were fitted to an exchange model²⁶ using unweighted non-linear regression,²⁷ further
 151 described in S10. The approach is similar for Altesil and SSP for which required K_{PW} of PRC, PeCB,
 152 HCB, PCB, and DDx are available in literature.²⁸⁻³¹ For BDE K_{PW} were only available for Altesil,
 153 which were used to derive K_{PW} for SSP as described in S9-4. Finally, $C_{P\rightleftharpoons\text{water}}$ were converted to lipid-
 154 basis ($C_{L\rightleftharpoons\text{water}}$) by multiplication with K_{LP} . All applied partition coefficients are collected in S11.

155

156 Results and discussion

157 **Trophic levels of the sampled fishes.** The $\delta^{15}\text{N}$ in fishes increase with their TL, but also differ
 158 between ecosystems, partly because of their dependence on the $\delta^{15}\text{N}$ at the base of the food chain.
 159 Therefore, the offset of $\delta^{15}\text{N}$ in the sampled fish species ($\delta^{15}\text{N}_{\text{fish tissue}}$) from $\delta^{15}\text{N}$ for primary
 160 producers or primary consumers ($\delta^{15}\text{N}_{\text{baseline}}$) is used to calculate TL:⁵

$$TL = (\delta^{15}N_{\text{fish tissue}} - \delta^{15}N_{\text{baseline}}) / \Delta^{15}N + TL_{\text{baseline}} \quad (3)$$

161 where the denominator $\Delta^{15}N$ represents the shift in $\delta^{15}N$ typical for one trophic level (3.4‰).³² To
 162 represent the primary consumers in the food webs, mussels (TL=2 by definition³²) were sampled and
 163 their $\delta^{15}N$ is applied as baseline ($\delta^{15}N_{\text{baseline}}$). At site A (fishpond), the $\delta^{15}N$ of swan mussels, small
 164 and larger duck mussels ranged between 10.87-12.62‰ and the lowest value (10.87‰ for the smallest
 165 duck mussels) was set as baseline assuming this to be the best representation, on the grounds that the
 166 higher $\delta^{15}N$ for the larger mussels may be a result of feeding on excretion of higher TL organisms.
 167 The $\delta^{15}N_{\text{mussel}}$ of 9.75‰ for swollen river mussels at site B was used as baseline for site B and C. The
 168 final TL values are listed in S12, together with the TL suggested at www.fishbase.org. The obtained
 169 TL ranges were 1.2–3.9, 2.3–3.6 and 3.2–3.5, for sites A, B and C, respectively.

170

171 Table 1 Mean ratio of lipid-based HOC^a concentrations by solvent extraction (Ext) and EPS in fish
 172 fillet and liver.

Ratios for:	Ext-liver	EPS-liver	EPS-fillet	EPS-liver
	Ext-fillet	EPS-fillet	Ext-fillet	Ext-liver
Ratio ^{a)}	0.98	1.13	1.02	1.18
sd ^{b)}	0.28	0.24	0.21	0.33
CI0.95 ^{c)}	0.05	0.04	0.04	0.06

173 a) Ratios for PeCB, HCB, PCB 28, 52, 101, 118,138, 153 and 180, and 4,4'-DDE.

174 b) standard deviation of the ratios

175 c) CI0.95 is 95% ± confidence range of the mean ratio

176

177 **Comparing C_L in fillet and liver by solvent extraction and EPS.** On average, C_L ratios between
 178 solvent extraction and EPS as well as between liver and fillet were close to unity (Table 1, S13) with
 179 the C_L in liver obtained by EPS being slightly higher on average (factor 1.18) than others. Although
 180 some ratios presented in Table 1 statistically differ from unity, the differences themselves were small
 181 when compared to differences in C_L occurring between the various species or even between different
 182 groups of the same species. For example, C_L values of all analyzed PCB ranged over a factor of 13

183 between the three asp fish groups from site B, while within each asp fish group the four C_L results by
184 solvent extraction and EPS in both fillet and liver were very similar, ranging within a factor 1.3 (S15).

185 Observing similar results for C_L and $C_{L\Rightarrow\text{fillet}}$ for fillets is in agreement with earlier work^{17,33} while
186 no application of EPS in liver was found in literature. The $C_{L\Rightarrow\text{liver}}$ being slightly higher than $C_{L\Rightarrow\text{fillet}}$
187 may be explained in various ways: (1) the applied lipid extraction method²³ was not validated for
188 liver tissue and possibly more than only lipid was extracted, resulting in underestimation of C_L , or (2)
189 during the two days tumbling for EPS, degradation of liver tissue could have occurred. This could
190 have reduced liver's HOC uptake capacity, resulting in a higher concentration in the sampler
191 enhancing $C_{L\Rightarrow\text{liver}}$. On the other hand, some thermodynamic gradient is required for HOC uptake in
192 the fish body. HOC's initial thermodynamic level in food increases in the gastrointestinal tract
193 because digestion reduces food's uptake capacity. The resulting higher thermodynamic level in food
194 processing organs drives the HOC distribution by the bloodstream to the fish body. This transport
195 direction is in agreement with the observation that $C_{L\Rightarrow\text{liver}}/C_{L\Rightarrow\text{fillet}}$ ratios larger than unity were
196 predominantly found in predatory fishes, e.g. wels catfish and perch (S14). The considerably higher
197 liver C_L as well as $C_{L\Rightarrow\text{liver}}$ for one of the wels catfish groups at site A (marked as WC-2 in S13)
198 corresponded with a much higher $\delta^{15}\text{N}$ in liver compared to fillet, while for most other fish samples
199 $\delta^{15}\text{N}$ in liver were mostly equal or lower than in fillet (S12).

200 The overall average factor 1.1 difference in C_L between fillet and liver indicates that the fast
201 pharmacokinetics of HOC quite efficiently limits differences in thermodynamic levels within the fish
202 body. The little differences between solvent extraction and EPS of fillet and liver, and probably also
203 whole fish, indicate that all methods can be interchangeably applied for monitoring of persistent HOC
204 in biota, provided that the results are expressed on lipid-basis.^{8,34}

205 For further evaluation, results by solvent extraction and EPS were averaged as analytical replicates
206 while fillet and liver were considered as two different samples having their own, sometimes different
207 $\delta^{15}\text{N}$. This approach provided 18 and 22 datapoints for sites A and B respectively, which were used
208 to compute TMF by linear regression of $\log C_L$ versus TL using eq (1). Regression results and

209 statistical parameters for site A and B are listed in S17. The fishes collected at site C were of similar
 210 TL (3.2-3.5), and, consequently, no TMF estimation was possible.

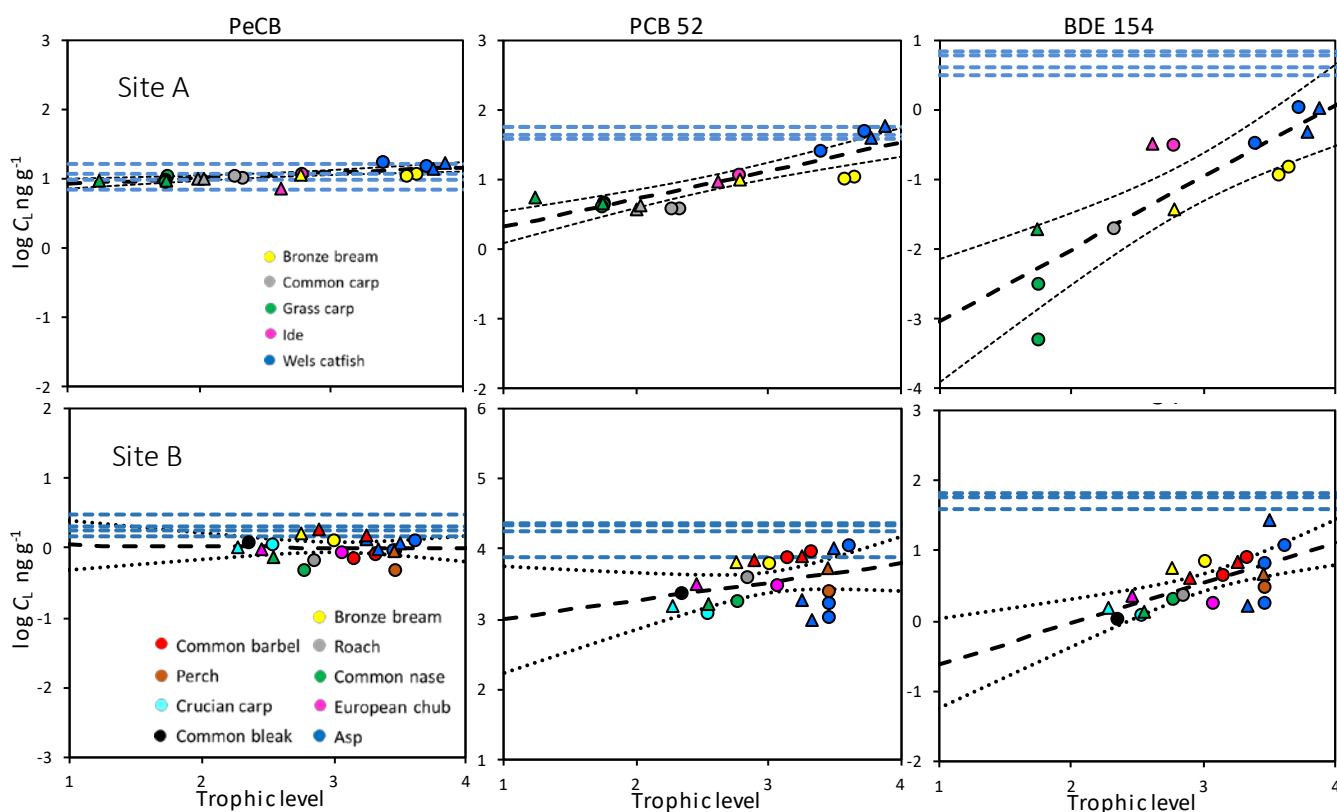


Fig. 1 Lipid-based concentrations (C_L) of three HOC of low, medium and high hydrophobicity in fillet (circles) and liver (triangles) versus the trophic level (TL) estimate at site A (upper row) and site B (lower row). Marker colors indicate fish species. The thick black dashed line represents the regression between C_L and TL (eq 1) and the dotted black lines indicate its upper and lower 95% confidence limits. The horizontal dashed blue lines represent the lipid-based concentrations for the water phase ($C_{L \rightleftharpoons \text{water}}$) as converted from equilibrium passive sampler (EPS) concentrations ($n=4$). The different lines indicate individual samplings.

211 **Trophic magnification factors (TMF).** The HOC's $\log C_L$ in the fish fillet and liver samples
 212 were nearly constant at all TL for PeCB while a positive $\log C_L$ -TL relation was observed for HOC
 213 of higher hydrophobicity (Fig. 1 and S16). The slope of this $\log C_L$ -TL relation equals $\log \text{TMF}$
 214 (eq 1), which increased as HOC's hydrophobicity increased. The resulting TMF exhibited a linear
 215 relationship with $\log K_{\text{OW}}$ for the persistent HOC, e.g. the PeCB, HCB and PCB (PCB-group), and
 216 most of the BDE (Fig. 2). The TMF- $\log K_{\text{OW}}$ relationship showed a steeper slope at site A compared
 217 to site B for the PCB group and, less pronounced for the BDE ($p>0.4$). The slope of the TMF- $\log K_{\text{OW}}$

218 relationships were higher for the BDE compared to the PCB group, indicating that, in addition to
219 hydrophobicity other unknown properties determine biomagnification. Note that the TMF for
220 BDE 99 is known to be affected by biotransformation³⁵ and its outlying value was therefore excluded
221 from regressions, as well as BDE 28, a biotransformation product of BDE 99.³⁵ BDE 47 is also a
222 biotransformation product of BDE 99 but because the BDE 47 concentration is two orders of
223 magnitude higher than BDE 28, an enhancement is not noticeable.

224 The high R^2 of TMF–log K_{ow} relationships (Fig. 2) confirm the effect of HOC's properties on
225 TMF but do not imply accuracy of the TMF themselves. The individual TMF are barely significant
226 when considering their 95% confidence ranges (see S18). This is because the effect of K_{ow} on the
227 TMF is the same for all species but TMF's uncertainty mainly arises from natural C_L variability
228 between fish species or fish groups (S15, S16). This variability is demonstrated in S19 where the
229 slopes of TMF–log K_{ow} relationships show to vary by a factor five when using all but one fish species,
230 i.e. for every line excluding a different fish species. Note that all regression lines in S19 closely
231 intercept at TMF=1 (PeCB). For site B, with more fish species, the TMF–log K_{ow} slope varies over
232 a factor of 2. A reason for the large TMF variability likely is that available species at the investigated
233 sites, although they belong to the same food web, may not be from a single food chain. Multiple food
234 chains, however, will be the reality in most river catchments.

235

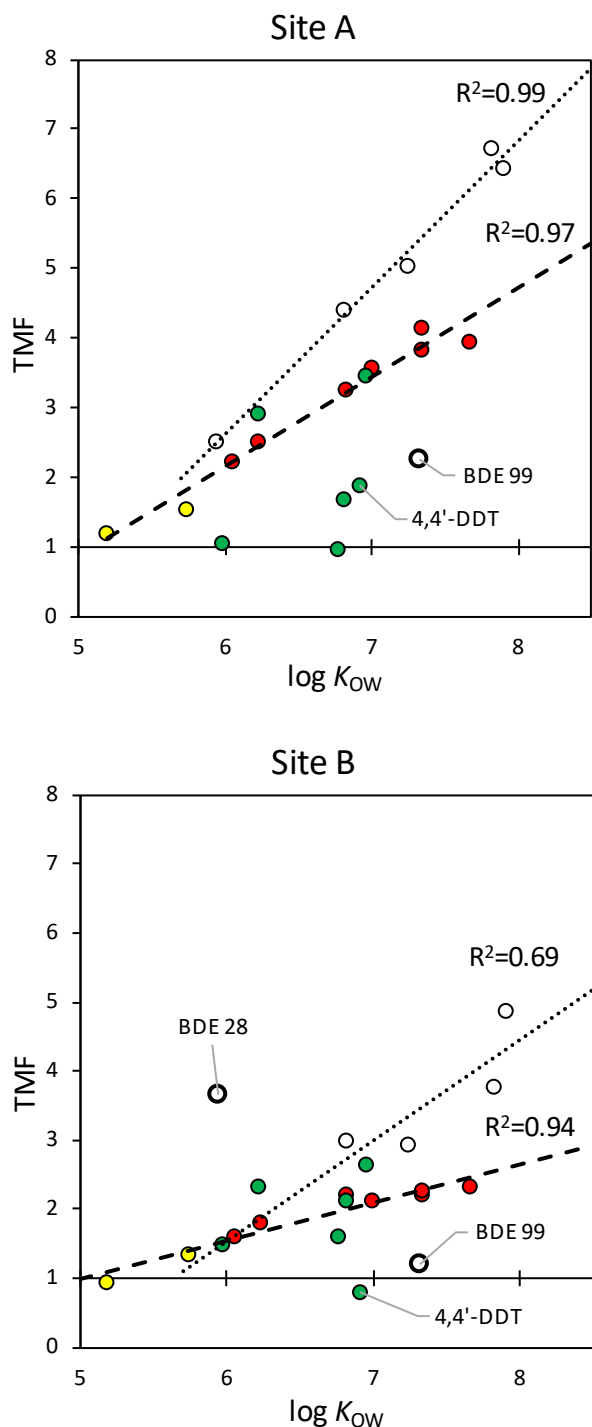


Fig. 2 Trophic magnification factors (TMF, y-axis) plotted versus $\log K_{ow}$ (x-axis) for PeCB and HCB (●), PCB (●), DDX (●) and BDE (○) for site A (upper panel) and B (lower panel). Dashed and dotted lines represent linear regression of TMF with $\log K_{ow}$ for PeCB, HCB plus PCB, and BDE (excluding bolded markers), respectively. DDX were not included in regression.

236

237 **HOC levels in fish and aqueous phase.** The observed C_L for PeCB in fishes were about equal at
 238 all TL and agreed well with $C_{L \rightleftharpoons water}$ (Fig. 1, left panels). However, as HOC's hydrophobicity

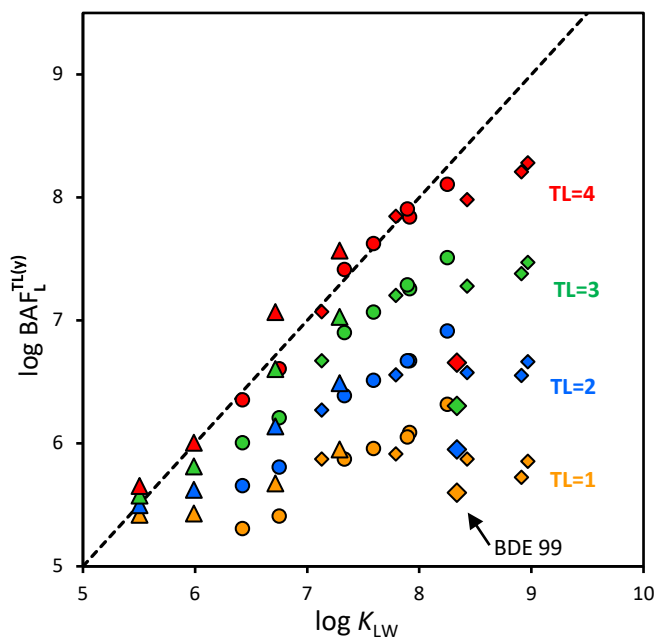
239 increased, their C_L in fishes at lower TL progressively decreased relative to $C_{L\rightleftharpoons\text{water}}$. This is visualized
 240 in S20 where the ratios between $C_L^{\text{TL}(y)}$ and $C_{L\rightleftharpoons\text{water}}$ of persistent HOC are plotted as a function of
 241 $\log K_{\text{OW}}$ for TL=y where y varies from 1 to 5. Using the regression data (eq 1) to set $C_L^{\text{TL}(y)}$ means that
 242 the data points represent a kind of average over all sampled fish species. The graphs in S20 show that
 243 at TL=1 the C_L could deviate from thermodynamic equilibrium with the water phase by three orders
 244 of magnitude for very high K_{OW} . With increasing TL C_L increased, getting to about the same level as
 245 $C_{L\rightleftharpoons\text{water}}$ at TL=4. This is not necessarily thermodynamic equilibrium and, assuming trophic
 246 magnification continues for organisms of TL>4, HOC's $C_L^{\text{TL}(>4)}/C_{L\rightleftharpoons\text{water}}$ ratio may exceed unity for
 247 HOC of $\log K_{\text{OW}} > \sim 6$.

248 It is illustrative to evaluate lipid-based bioaccumulation factors ($\text{BAF}_L^{\text{TL}(y)}$) at specific TL values.
 249 $\text{BAF}_L^{\text{TL}(y)}$ are calculated as:

$$\text{BAF}_L^{\text{TL}(y)} = \frac{C_L^{\text{TL}(y)}}{C_w} \quad (4)$$

250 where C_w were estimated from passive sampling as described in S10. $\log \text{BAF}_L^{\text{TL}(y)}$ are plotted versus
 251 \log lipid–water partition coefficients ($\log K_{\text{LW}}$, S11) in Fig. 3, showing an increasing deviation from
 252 K_{LW} for TL<4 (vertical) and hydrophobicity increases (horizontal). The $\log \text{BAF}$ – $\log K_{\text{LW}}$ or $\log K_{\text{OW}}$
 253 relationships leveling off at higher hydrophobicity ($\log K_{\text{OW}} > 5$ or 6) is frequently reported in
 254 literature and has been associated with a corresponding larger molecular size, which would limit its
 255 membrane passage.³⁶ However, a molecular size effect was not supported by analysis of a large
 256 amount of literature data³⁷ and often can be explained by other factors, including measurement
 257 artefacts or non-equilibrium with the surrounding environment³⁸ and is also shown here.

258



259

260 Fig. 3 Lipid-based bioaccumulation factors ($BAF_L^{TL(y)}$) in fishes at site A are plotted versus K_{LW} for
 261 different trophic levels (TL). $BAF_L^{TL(y)}$ were calculated as the ratio of the lipid-based concentration at
 262 $TL=y$ ($C_L^{TL(y)}$) and the aqueous concentrations obtained by passive sampling (C_w) as described in S10.
 263 The $C_L^{TL(y)}$ in fishes at $TL(y)$ for $y=1$ to 4 (1orange, 2blue, 3green and 4red) were obtained from
 264 regression using eq (1) and are actually points on the regression lines in Fig. 1 at the respective $TL(y)$.
 265 The dashed line indicates equality between $\log BAF$ and $\log K_{LW}$. Symbol shapes indicate (Δ) Penta-
 266 and hexa-chlorobenzene, 4,4'-DDD and 4,4'-DDE, (\circ) PCB and (\diamond) BDE.

267

268 **Thermodynamic level difference between fishes and the water phase.** The much lower C_L
 269 compared to $C_{L \rightleftharpoons water}$ at $TL=1$ for high K_{OW} HOC strongly indicate that HOC levels at the bottom of
 270 the food web, phytoplankton e.g. algae, are not at thermodynamic equilibrium with the water phase.
 271 Evaluation of long-term PCB monitoring in herring gull eggs showed that occasionally lower PCB
 272 levels corresponded to seasons with favorable conditions for algal growth, demonstrating how a lack
 273 of equilibrium can affect levels higher in the food chain.³⁹ This is not consistent with exposure of
 274 algae to PCB in laboratory conditions, for which equilibration times of one hour,⁴⁰ several hours,⁴¹
 275 or a day⁴² were observed, while for PCB of $K_{OW} > 10^6$ also non-equilibrium after a week of exposure
 276 was reported⁴³. Other studies report equilibrium attainment of phytoplankton in the laboratory and
 277 the field.^{44,45}

278 At equilibrium, the ratio between the concentration in algae (C_A) and C_W is given by the
 279 bioconcentration factor (BCF). Evaluating equilibrium attainment, it should be realized that primary
 280 producers such as phytoplankton, phytobenthos, macrophytes dominantly grow from photosynthetic
 281 carbon dioxide assimilation and inorganic nutrients. Because these components do not contain HOC,
 282 in first instance HOC concentrations in algal cells are minimal and HOC are taken up from the
 283 aqueous phase by diffusion through an aqueous boundary layer at the surface (WBL) and a cell wall
 284 or a membrane. Previously published models of PCB uptake by phytoplankton and bacteria were not
 285 consistent whether the mass transfer is controlled by the biological membrane⁴⁶ or the WBL.⁴⁷ Here
 286 it is important to stress that the mass transfer rate is determined by the product of diffusion coefficient
 287 and solubility,⁴⁸ i.e. the permeability. Since the BCF also reflects the ratio between solubility of an
 288 HOC in an organism and the aqueous phase, slower diffusion in biological material is compensated
 289 by a higher solubility than in water, resulting in a high permeability. Consequently, for HOC's of
 290 higher hydrophobicity, mass transport in the WBL controls the uptake rate. Additionally, the WBL
 291 at the surface of, or actually around the algal cells, is generally much thicker than the biological
 292 membrane. Consequently, acknowledging that the transport resistance is dominated by the WBL, the
 293 HOC uptake process of primary producers (further referred to as "algae") can be modeled analogously
 294 to passive samplers.

295 **Algal HOC uptake modeled as passive sampling.** Passive samplers exposed in the laboratory
 296 in a defined volume of aqueous HOC solution equilibrate much faster than when exposed in field
 297 conditions.⁴⁹ This is due to the dependence of the first order kinetic rate constant on the ratio of the
 298 sorbent capacity and the water volume used.⁵⁰ For WBL controlled partition PS, a model for HOC
 299 uptake by a PS from a defined volume of contaminated water is available from Booij et al,⁵¹ which
 300 was adapted to provide HOC concentrations in algae (C_A^t , ng kg⁻¹) as a function of exposure time
 301 (t , d):

$$C_A^t = \frac{C_W^0 \text{BCF} \left\{ 1 - \exp \left[- \left(1 + \frac{m_A \text{BCF}}{V_W} \right) \frac{k_w A_A}{m_A \text{BCF}} t \right] \right\}}{1 + \frac{m_A \text{BCF}}{V_W}} \quad (5)$$

302 where C_w^0 is the dosed HOC concentration in the aqueous solution (ng L^{-1}) at $t=0$ and a volume V_w
 303 (L), the BCF (L kg^{-1}) HOC's bioconcentration factor in algae (replacing K_{pw}), m_A the algae mass
 304 (kg), k_w the mass transfer coefficient in the WBL (dm d^{-1}), and A_A the total surface area of the algae
 305 (dm^2). Similarly, the time course of the aqueous concentration (C_w^t) is given by:⁵¹

$$C_w^t = \frac{C_w^0 \left\{ 1 + \frac{m_A \text{BCF}}{V_w} \exp \left[- \left(1 + \frac{m_A \text{BCF}}{V_w} \right) \frac{k_w A_A}{m_A \text{BCF}} t \right] \right\}}{1 + \frac{m_A \text{BCF}}{V_w}} \quad (6)$$

306 Note that in these equations the exponent equals $-k_e t$, wherein k_e (d^{-1}) is the first order exchange
 307 rate constant. Consequently, k_e is higher if $m_A \text{BCF}/V_w$ (L L^{-1}) is high, explaining the fast
 308 equilibration when sorbent capacity ($m_A \text{BCF}$; in L) of the algae is much larger than the water volume
 309 V_w (L). Opposite, when V_w is infinitely large, as is the case in field conditions, $m_A \text{BCF}/V_w \rightarrow 0$ and
 310 eq (5) reduces to:

$$C_A^t = C_w^0 \text{BCF} \left\{ 1 - \exp \left[- \frac{k_w A_A}{\text{BCF } m_A} t \right] \right\} \quad (7)$$

311 In such situation C_w^t remains constants and equal to C_w^0 .

312 Using these models, C_A^t and C_w^t were modeled as a function of time for three cases involving HOC
 313 uptake by a same algal mass ($\sim 25 \times 10^{-6}$ kg) where (I) $V_w = 0.05$ L and $A_A = 10$ dm^2 by Sijm et al,⁴⁰
 314 (II) $V_w = 1$ L and $A_A = 16$ dm^2 by Koelmans et al⁴² and (III) $V_w = \infty$ (field situation) and $A_A = 10$ dm^2 ,
 315 assuming a hypothetical situation that algae do not grow (see S21-1 for more detail). An average k_w
 316 of $0.1 \mu\text{m s}^{-1}$ (0.09 dm d^{-1}) was derived by fitting k_e to the rate constants reported for the cases (I)⁴⁰
 317 and (II).⁴² This k_w was used in all three cases providing sampling rates ($R_s = k_w A_A$) of 0.86, 1.35 and
 318 0.86 L d^{-1} , for (I), (II) and (III), respectively.

319 **Modeling results: laboratory versus field.** Modeling showed that equilibration times for HOC
 320 observed in laboratory conditions generally do not apply to the field situation and are expected to
 321 increasingly deviate with increasing BCF. Modeling C_A^t and C_w^t profiles versus time for HOC of
 322 log BCF 3 to 8, showed that algae equilibrate in less than a day at laboratory conditions where a
 323 limited water volume is applied (S21-2 and S21-3), while in the field for HOC of log BCF 5 to 8
 324 equilibration times of 10 to 10000 days would apply (S21-4).

325 To evaluate and explain this, instead of full equilibrium requiring infinite time, we calculated the
 326 time at which C_A^t and C_W^t are within 10% of their final equilibrium values, i.e. t_A^{90} and t_W^{90} for algae
 327 and water phase, respectively (S21). These timepoints are marked in S21-2 and S21-3, and listed in
 328 S22. For all three cases these t^{90} are plotted versus log BCF in Fig. 4, applying a logarithmic and a
 329 temporal scale in panel A and B, respectively. Panel A in Fig. 4 shows that for the field situation (III),
 330 t_A^{90} increases proportionally to BCF. The t_A^{90} exceeds the lifespan of algae at log BCF 4.5 to 5, which
 331 is evident when t^{90} are plotted at a linear scale (Fig. 4, panel B). In contrast, t_A^{90} is relatively short in
 332 laboratory exposures and constant when log BCF is higher than 4 and 5 for case (I), $V_w=0.05$ L and
 333 case (II), $V_w=1$ L, respectively. This is because for equilibration in a defined water volume with
 334 $m_A \text{BCF}/V_w \gg 1$, t_A^{90} is determined by V_w , rather than BCF.⁴⁰

335 For the aqueous phase, the profiles in panel A of Fig. 4 and S21-2 and S21-3, show that towards
 336 higher BCF, t_W^{90} becomes increasingly larger than t_A^{90} . The t_W^{90} equals t_A^{90} when $m_A \text{BCF}/V_w=1$ and for
 337 higher ratios the relative difference between t_W^{90} and t_A^{90} is determined by the phase capacity factor
 338 $\log(m_A \text{BCF}/V_w)$, by which C_w has to decrease to attain a level within 10% from equilibrium:

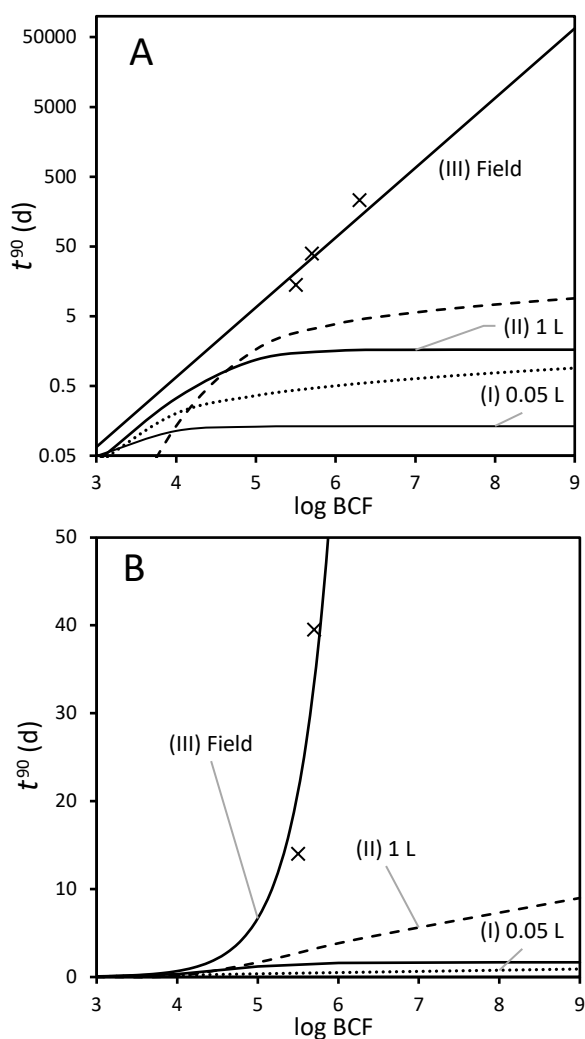
$$\frac{t_W^{90}-t_A^{90}}{t_A^{90}} = \log\left(\frac{\text{BCF } m_A}{V_w}\right) \quad \text{and} \quad t_W^{90} = t_A^{90} \log\left(\frac{\text{BCF } m_A}{V_w}\right) + t_A^{90} \quad (8)$$

339 Note that this equation fails if the algal uptake does not affect C_w^0 by more than 10%, i.e. $t_W^{90}=0$.

340 In the graphs in S21-2 and S21-3, the extent C_w at t_A^{90} is higher than C_w at t_W^{90} is shown by the
 341 length of a vertical line. At a log BCF of 7 the ratio $C_w(t_A^{90})/C_w(t_W^{90})$ amounts 6000 and 250 for case
 342 (I) and (II), respectively. Although this factor is higher when V_w is very small, the phenomenon is
 343 more relevant for larger V_w because of the associated longer absolute time between t_A^{90} and t_W^{90} . The
 344 extent t_W^{90} is longer than t_A^{90} , is relevant for in laboratory BCF estimations, where equilibrium
 345 attainment is generally assessed by monitoring the concentration in the algae. Ending exposure earlier
 346 than t_W^{90} causes an increasing underestimation of BCF towards HOC of higher hydrophobicity. Such
 347 underestimation may contribute to the log BCF–log K_{ow} relation for algae leveling off around
 348 $\log K_{ow} \approx 6^{43}$. We write “contributing”, as such effect is indistinguishable from overestimation of

349 aqueous concentrations by insufficiently excluding HOC fractions bound to DOC or exudate when
 350 quantifying C_w .

351



352

353 Fig. 4 Modeled time required for algae to attain the concentration within 10% equilibrium (t^{90})
 354 for three cases where $\sim 25 \times 10^{-6}$ kg algae was exposed to (I) 0.05 L,⁴⁰ (II) 1 L,⁴² or (III) infinite volume
 355 of water, plotted versus log BCF with the y-axis at a logarithmic scale (panel A) and at a linear scale
 356 for 0–50 days (panel B). Solid and dashed lines indicate the t^{90} for algal uptake and water phase
 357 decrease, respectively. In the field the aqueous concentration was considered constant and t_w^{90} does
 358 not apply. The (x) markers represent experimental t^{90} from gas purge elimination of three PCB
 359 congeners by Koelmans et al.⁴²

360

361 **Evaluation of model application.** When applying passive sampling theory for modeling WBL
 362 controlled algal uptake, the key parameter is the mass transfer coefficient (k_w) which depends on the

363 water turbulence near the algal surface. The k_w derived above corresponds to a sampling rate of 0.09
364 $L d^{-1} dm^{-2}$, which is very low compared to what is observed for passive sampling, where even in
365 quiescent conditions sampling rates are commonly higher by more than an order of magnitude.
366 However, the position of a passive sampler is typically fixed in the water current, whereas algae float
367 in/with the streaming water and may reside in the same water causing a thick water boundary layer
368 and low k_w . Except for algae growing on rocks, there is no reason to believe that k_w in field would be
369 higher than estimated for stirred laboratory exposures, and the timescale of the modeled equilibration
370 times (Fig.4) for HOC of higher hydrophobicity ($\log BCF > 5$) can be considered realistic. Due to the
371 long equilibration timescale for HOC of high $\log K_{OW}$, combined with an inevitable algal growth, it
372 is not feasible to validate the model results in field conditions. However, elimination rate estimation
373 in the laboratory by gas purging of HOC simulates an aqueous phase of infinite size.⁴² Assuming that,
374 similar to WBL controlled passive sampling, the algal uptake process is also isotropic, the elimination
375 process of HOC from dosed algae mirrors the uptake process. Inserting the t^{90} release times from the
376 gas purge elimination curves by Koelmans et al⁴² in Fig. 4 shows that these are in good agreement
377 with the t_A^{90} modeled for field uptake by algae. This observation supports that laboratory results can
378 be used to predict passive uptake using the presented modeling approach. In field conditions, both
379 slow HOC uptake and growth dilution are the main obstacles that prevent algae to achieve the same
380 thermodynamic levels as the aqueous phase. Consumer organisms on the other hand, take up HOC
381 via food, which is only partly converted to biomass. The accumulation from food uptake, together
382 with respiratory uptake, increases HOC's concentration more than growth dilution will decrease it.
383 Accumulation above the thermodynamic level of the aqueous phase will end when the respiratory
384 HOC flux driven by a thermodynamic gradient between the organism and the water phase, equals the
385 uptake by the food route.

386 **Implications.** The C_L in fishes of TL <4 being lower than $C_{L \rightleftharpoons water}$ is not compatible with the
387 general belief that trophic magnification typically amplifies levels of persistent HOC in e.g. fish
388 above that of the surrounding environment. Although C_L in fish and invertebrates being lower than
389 $C_{L \rightleftharpoons water}$ or $C_{L \rightleftharpoons sediment}$, has been frequently observed,^{10,12-14,52} possible reasons, including the above,

390 were discussed without firm conclusions, except that $C_{L\rightleftharpoons\text{water}}$ and $C_{L\rightleftharpoons\text{sediment}}$ are useful in
391 bioaccumulation research and a viable alternative to chemical monitoring in biota. The latter could
392 apply for the OSPAR Coordinated Environmental Monitoring Program (CEMP)² or the chemical
393 biota monitoring under the WFD.¹ Differences in concentrations in fishes of different TL were
394 recognized by the WFD requiring compliance to Environmental Quality Standards (EQS) of priority
395 substances in fishes at TL=4, and if such fishes are not available, inter- or extrapolation (eq 1) has to
396 be applied using data of available fish species.⁵ The necessary TMF are ecosystem, food web and
397 HOC-specific. Guidance is provided for selecting and determination of TMF for application under
398 the EU WFD,⁴ but it could not be resolved which TMF would apply to the river systems and the
399 fishpond in this study. The most robust way to correct for trophic magnification is in-situ TMF
400 determination, i.e. regressing HOC's $C_L^{\text{TL}(x)}$ measured in various sampled fish species versus TL,
401 preferably comprising at least two TL units.⁴ Nevertheless, the $C_L^{\text{TL}(4)}$ resulting from extrapolation at
402 site A and B, each using twenty fish samples, on average showed a two times larger 95% confidence
403 range compared to $C_{L\rightleftharpoons\text{water}}$ for which four samplings were performed (S24, S25). Apart from the 95%
404 confidence range $C_L^{\text{TL}(4)}$ may still be biased if by chance the sampled fish species are not from the
405 same food chain and/or the reference $\delta^{15}\text{N}$ as well as the 3.4 ‰ for $\Delta^{15}\text{N}$ do not apply for the local
406 situation. The concept of PS, on the other hand, is straightforward. PS essentially adds an artificial
407 medium (a polymeric sampler of constant properties without biotransformation) to the ecosystem.
408 The accuracy of $C_{L\rightleftharpoons\text{water}}$ relates to uncertainties of HOC quantification in the sampler, polymer–water
409 and lipid–sampler partition coefficients, and to that of the model used for in-situ sampler calibration.
410 The partition coefficients are physical constants that have no natural variability and are as accurate
411 as analytically determined. Moreover, $C_{L\rightleftharpoons\text{water}}$ also is a better reflection of the actual HOC exposure
412 of organisms, as HOC's C_L may be reduced or diminished due to bio-transformation in fish, e.g. some
413 DDX and BDE 99, while the exposure to HOC undetected in the tissue may have harmed the
414 organism. To bridge both approaches it was suggested to routinely apply PS and, in case the EQS is
415 approached or exceeded, apply chemical monitoring in biota.⁵³

416 For HOC of $K_{ow} > 10^6$, uptake and equilibration rates for primary producers need further attention
417 and such research should include the use of PS and/or passive dosing. Moreover, the thermodynamic
418 levels for HOC in primary producers and primary consumers being lower than in the aqueous phase
419 need to be considered when setting the food chain/web bottom reference point in modeling of real
420 field conditions with realistic growth.

421

422 The authors declare no competing financial interest.

423

424 **Supporting information**

425 Supporting information contains additional procedure descriptions, tables and figures presented
426 in the order they are referred to in the text. This information is available free of charge via the internet
427 at <http://pubs.acs.org>.

428 **Acknowledgements**

429 This work was supported by the Czech Science Foundation grant No. GACR 15-16512S
430 “Investigation of accumulation of persistent bioaccumulative toxic organic substances into aquatic
431 organisms”. The research activities were carried out in the RECETOX Research Infrastructure
432 supported by the Czech Ministry of Education, Youth and Sports (LM2015051) and the European
433 Structural and Investment Funds, Operational Programme Research, Development, Education
434 (CZ.02.1.01/0.0/0.0/16_013/0001761). We thank Petra Příbylová, Petr Kukučka, Jakub Martiník,
435 Ondřej Audy, Krzysztof Okonski and Roman Prokeš from RECETOX, Masaryk University for their
436 assistance with sampling, sample preparation and instrumental analysis of samples and Ondřej Sáňka
437 from RECETOX, Masaryk University for his assistance with the preparation of maps. We also thank
438 Dr. Daniel Grul'a and his colleagues from the ichthyological survey company ARAR s.r.o. and Dr.
439 Pavel Jurajda and his colleagues from the Institute of Vertebrate Biology of the Czech Academy of
440 Sciences for providing fish samples for the study from the Laborec and Bečva rivers. Advice of an
441 unknown reviewer was highly appreciated.

442

443 **Literature cited**

- 444 1 EU WFD Directive 2013/39/EU of the European Parliament and of the Council of 12 August
445 2013 amending Directives 2000/60/EC and 2008/105/EC as regards priority substances in the
446 field of water policy. *Off. J. Eur. Union* **2013**, L226, 1-17.
- 447 2 OSPAR Coordinated Environmental Monitoring Programme (CEMP), OSPAR Agreement
448 2016-01, updated 2018. **2016**, <http://www.ospar.org/documents?d=32943>
- 449 3 OSPAR Background Document on CEMP assessment criteria for the QSR 2010. **2009**,
450 *Document nr: 461/209; ISBN 978-1-907390-08-1;*
451 [https://qsr2010.ospar.org/media/assessments/p00390_supplements/p00461_Background_Doc_](https://qsr2010.ospar.org/media/assessments/p00390_supplements/p00461_Background_Doc_CEMP_Assessmt_Criteria_Haz_Subst.pdf)
452 [CEMP_Assessmt_Criteria_Haz_Subst.pdf](https://qsr2010.ospar.org/media/assessments/p00390_supplements/p00461_Background_Doc_CEMP_Assessmt_Criteria_Haz_Subst.pdf)
- 453 4 Kidd, K.A.; Burkhard, L.P.; Babut, M.; Borgå, K.; Muir, D.C.G.; Perceval, O.; Ruedel, H.;
454 Woodburn, K.; Embry, M.R. Practical advice for selecting or determining trophic magnification
455 factors for application under the European Union Water Framework Directive. *Integr. Environ.*
456 *Assess. Manag.* **2018**, 15 266-277; DOI 10.1002/ieam.4102
- 457 5 Deutsch, K.; Leroy, D.; Belpaire, C.; den Haan, K.; Vrana, B.; Clayton, H.; Hanke, G.; Ricci,
458 M.; Held, A.; Gawlik, B.; Babut, M.; Perceval, O.; Lepom, P.; Heiss, C.; Koschorreck, J.;
459 O'Toole, S.; Valsecchi, S.; Polesello, S.; Carere, M.; ten Hulscher, D.; Verbruggen, E.; Dulio,
460 V.; Green, N.; Viñas, L.; Bellas, J.; Lilja, K.; Bignert, A.; Whitehouse, P.; Sumner, K.; Law, R.;
461 Brant, J.; Leverett, D.; Merrington, G. Guidance document no. 32 on biota monitoring (the
462 implementation of EQS biota) under the water framework directive. *Common Implementation*
463 *Strategy for the Water Framework Directive (2000/60/EC)* **2014**, Technical Report - 2014 - 083
464 DOI: 10.2779/833200
- 465 6 OSPAR CEMP Guidelines for Monitoring Contaminants in Biota (updated 2018). **1999**,
466 <https://www.ospar.org/convention/agreements?q=1999-02&t=&a=&s=>
- 467 7 Fliedner, A.; Rüdell, H.; Teubner, D.; Buchmeier, G.; Lowis, J.; Heiss, C.; Wellmitz, J.;
468 Koschorreck, J. Biota monitoring and the Water Framework Directive---can normalization

- 469 overcome shortcomings in sampling strategies? *Environ. Sci. Pollut. Res.* **2016**, *23*, 21927-
470 21939; DOI 10.1007/s11356-016-7442-2"
- 471 8 Fliedner, A.; Rüdell, H.; Lohmann, N.; Buchmeier, G.; Koschorreck, J. Biota monitoring under
472 the Water Framework Directive: On tissue choice and fish species selection. *Environ. Pollut.*
473 **2018**, *235*, 129-140; DOI 10.1016/j.envpol.2017.12.052
- 474 9 Khairy, M.A.; Noonan, G.O.; Lohmann, R. Uptake of hydrophobic organic compounds,
475 including organochlorine pesticides, polybrominated diphenyl ethers, and perfluoroalkyl acids in
476 fish and blue crabs of the lower Passaic River, New Jersey, USA. *Environ. Toxicol. Chem.* **2019**,
477 *38*, 872-882; DOI 10.1002/etc.4354
- 478 10 Mäenpää, K.; Leppänen, M.; Figueiredo, K.; Mayer, P.; Gilbert, D.; Jahnke, A.; Gil-Allué, C.;
479 Akkanen, J.; Nybom, I.; Herve, S. Fate of polychlorinated biphenyls in a contaminated lake
480 ecosystem: combining equilibrium passive sampling of sediment and water with total
481 concentration measurements of biota. *Environ. Toxicol. Chem.* **2015**, *34*, 2463-2474; DOI
482 10.1002/etc.3099
- 483 11 Reichenberg, F.; Smedes, F.; Jonsson, J.; Mayer, P. Determining the chemical activity of
484 hydrophobic organic compounds in soil using polymer coated vials. *Chem. Cent. J.* **2008**, *2*, 8;
485 DOI 10.1186/1752-153X-2-8
- 486 12 Jahnke, A.; Mayer, P.; McLachlan, M.S.; Wickstrom, H.; Gilbert, D.; MacLeod, M. Silicone
487 passive equilibrium samplers as 'chemometers' in eels and sediments of a Swedish lake. *Environ.*
488 *Sci. Processes Impacts* **2014**, *16*, 464-472; DOI 10.1039/C3EM00589E
- 489 13 Jahnke, A.; MacLeod, M.; Wickstrom, H.; Mayer, P. Equilibrium sampling to determine the
490 thermodynamic potential for bioaccumulation of persistent organic pollutants from sediment.
491 *Environ. Sci. Technol.* **2014**, *48*, 11352-11359; DOI 10.1021/es503336w
- 492 14 Figueiredo, K.; Mäenpää, K.; Lyytikäinen, M.; Taskinen, J.; Leppänen, M.T. Assessing the
493 influence of confounding biological factors when estimating bioaccumulation of PCBs with
494 passive samplers in aquatic ecosystems. *Sci. Total Environ.* **2017**, *601-602*, 340-345; DOI
495 10.1016/j.scitotenv.2017.05.140

- 496 15 Figueiredo, K.; Mäenpää, K.; Leppänen, M.T.; Kiljunen, M.; Lyytikäinen, M.; Kukkonen,
497 J.V.K.; Koponen, H.; Biasi, C.; Martikainen, P.J. Trophic transfer of polychlorinated biphenyls
498 (PCB) in a boreal lake ecosystem: Testing of bioaccumulation models. *Sci. Total Environ.* **2014**,
499 466–467, 690-698; DOI 10.1016/j.scitotenv.2013.07.033
- 500 16 Jahnke, A.; Mayer, P.; Adolfsson-Erici, M.; McLachlan, M.S. Equilibrium sampling of
501 environmental pollutants in fish: comparison with lipid-normalized concentrations and
502 homogenization effects on chemical activity. *Environ. Toxicol. Chem.* **2011**, 30, 1515-1521; DOI
503 10.1002/etc.534
- 504 17 Rusina, T.P.; Carlsson, P.; Vrana, B.; Smedes, F. Equilibrium passive sampling of POP in lipid-
505 rich and lean fish tissue: quality control using performance reference compounds. *Environ. Sci.*
506 *Technol.* **2017**, 51, 11250-11257; DOI 10.1021/acs.est.7b03113
- 507 18 Mäenpää, K.; Leppänen, M.T.; Reichenberg, F.; Figueiredo, K.; Mayer, P. Equilibrium sampling
508 of persistent and bioaccumulative compounds in soil and sediment: comparison of two
509 approaches to determine equilibrium partitioning concentrations in lipids. *Environ. Sci. Technol.*
510 **2011**, 45, 1041-1047; DOI 10.1021/es1029969
- 511 19 Smedes, F.; Booij, K. Guidelines for passive sampling of hydrophobic contaminants in water
512 using silicone rubber samplers. *ICES Techniques in Marine Environmental Sciences* **2012**, No.
513 52 (20pp); DOI:10.17895/ices.pub.5077
- 514 20 Vrana, B.; Smedes, F.; Allan, I.; Rusina, T.; Okonski, K.; Hilscherová, K.; Novák, J.; Tarábek,
515 P.; Slobodník, J. Mobile dynamic passive sampling of trace organic compounds: Evaluation of
516 sampler performance in the Danube River. *Sci. Total Environ.* **2018**, 636, 1597-1607; DOI
517 10.1016/j.scitotenv.2018.03.242
- 518 21 Vrana, B.; Rusina, T.; Okonski, K.; Prokeš, R.; Carlsson, P.; Kopp, R.; Smedes, F. Chasing
519 equilibrium passive sampling of hydrophobic organic compounds in water. *Sci. Total Environ.*
520 **2019**, 664, 424-435; DOI 10.1016/j.scitotenv.2019.01.242

- 521 22 Kocan, A.; Petrik, J.; Jursa, S.; Chovancova, J.; Drobna, B. Environmental contamination with
522 polychlorinated biphenyls in the area of their former manufacture in Slovakia. *Chemosphere*
523 **2001**, 43, 595-600; DOI 10.1016/S0045-6535(00)00411-2
- 524 23 Smedes, F. Determination of total lipid using non-chlorinated solvents. *Analyst* **1999**, 124, 1711-
525 1718; DOI 10.1039/a905904k
- 526 24 Smedes, F.; Rusina, T.P.; Beeltje, H.; Mayer, P. Partitioning of hydrophobic organic
527 contaminants between polymer and lipids for two silicones and low density polyethylene.
528 *Chemosphere* **2017**, 186, 948-957; DOI 10.1016/j.chemosphere.2017.08.044
- 529 25 Jahnke, A.; McLachlan, M.S.; Mayer, P. Equilibrium sampling: Partitioning of organochlorine
530 compounds from lipids into polydimethylsiloxane. *Chemosphere* **2008**, 73, 1575-1581; DOI
531 10.1016/j.chemosphere.2008.09.017
- 532 26 Rusina, T.P.; Smedes, F.; Koblizkova, M.; Klanova, J. Calibration of silicone rubber passive
533 samplers: experimental and modeled relations between sampling rate and compound properties.
534 *Environ. Sci. Technol.* **2010**, 44, 362-367; DOI 10.1021/es900938r
- 535 27 Booij, K.; Smedes, F. An Improved method for estimating in situ sampling rates of nonpolar
536 passive samplers. *Environ. Sci. Technol.* **2010**, 44, 6789-6794; DOI 10.1021/es101321v
- 537 28 Smedes, F.; Geertsma, R.W.; van der Zande, T.; Booij, K. Polymer-water partition coefficients
538 of hydrophobic compounds for passive sampling: application of cosolvent models for validation.
539 *Environ. Sci. Technol.* **2009**, 43, 7047-7054; DOI 10.1021/es9009376
- 540 29 Smedes, F. Silicone–water partition coefficients determined by cosolvent method for chlorinated
541 pesticides, musks, organo phosphates, phthalates and more. *Chemosphere* **2018**, 210, 662-671;
542 DOI 10.1016/j.chemosphere.2018.07.054
- 543 30 Smedes, F. Corrigendum to “Silicone–water partition coefficients determined by cosolvent
544 method for chlorinated pesticides, musks, organo phosphates, phthalates and more”
545 [Chemosphere 210 (2018) 662–671]. *Chemosphere* **2018**, 212, 1180; DOI
546 10.1016/j.chemosphere.2018.09.094 "

- 547 31 Smedes, F. SSP silicone-, lipid- and SPMD-water partition coefficients of seventy hydrophobic
548 organic contaminants and evaluation of the water concentration calculator for SPMD.
549 *Chemosphere* **2019**, 223, 748-757; DOI 10.1016/j.chemosphere.2019.01.164
- 550 32 Post, D.M. Using stable isotopes to estimate trophic position: models, methods, and assumptions.
551 *Ecology* **2002**, 83, 703-718; DOI 10.1890/0012-9658(2002)083[0703:USITET]2.0.CO;2
- 552 33 Jahnke, A.; Mayer, P.; Broman, D.; McLachlan, M.S. Possibilities and limitations of equilibrium
553 sampling using polydimethylsiloxane in fish tissue. *Chemosphere* **2009**, 77, 764-770; DOI
554 10.1016/j.chemosphere.2009.08.025
- 555 34 Schneider, R. Polychlorinated biphenyls (PCBs) in cod tissues from the Western Baltic:
556 significance of equilibrium partitioning and lipid composition in the bioaccumulation of
557 lipophilic pollutants in gill-breathing animals. *Meeresforsch.* **1982**, 29, 69-79.
- 558 35 Noyes, P.D.; Kelly, S.M.; Mitchelmore, C.L.; Stapleton, H.M. Characterizing the in vitro hepatic
559 biotransformation of the flame retardant BDE 99 by common carp. *Aquat. Toxicol.* **2010**, 97,
560 142-150; DOI 10.1016/j.aquatox.2009.12.013
- 561 36 Opperhuizen, A.; van der Velde, E.W.; Gobas, F.A.P.C.; Liem, D.A.K.; van der Steen, J.M.D.
562 Relationship between bioconcentration in fish and steric factors of hydrophobic chemicals.
563 *Chemosphere* **1985**, 14, 1871-1896; DOI 10.1016/0045-6535(85)90129-8
- 564 37 Arnot, J.A.; Arnot, M.I.; Mackay, D.; Couillard, Y.; MacDonald, D.; Bonnell, M.; Doyle, P.
565 Molecular size cutoff criteria for screening bioaccumulation potential: Fact or fiction? *Integr.*
566 *Environ. Assess. Manag.* **2010**, 6, 210-224; DOI 10.1897/IEAM_2009-051.1
- 567 38 Jonker, M.T.O.; van der Heijden, S.A. Bioconcentration factor hydrophobicity cutoff: an
568 artificial phenomenon reconstructed. *Environ. Sci. Technol.* **2007**, 41, 7363-7369; DOI
569 10.1021/es0709977
- 570 39 Smith, D. Synchronous response of hydrophobic chemicals in herring gull eggs from the Great-
571 Lakes. *Environ. Sci. Technol.* **1995**, 29, 740-750; DOI 10.1021/es00003a023

- 572 40 Sijm, D.; Broersen, K.; de Roode, D.; Mayer, P. Bioconcentration kinetics of hydrophobic
573 chemicals in different densities of *Chlorella pyrenoidosa*. *Environ. Toxicol. Chem.* **1998**, *17*,
574 1695-1704; DOI 10.1002/etc.5620170908
- 575 41 Gerofke, A.; Komp, P.; McLachlan, M. Bioconcentration of persistent organic pollutants in four
576 species of marine phytoplankton. *Environ. Toxicol. Chem.* **2005**, *24*, 2908-2917; DOI
577 10.1897/04-566R.1
- 578 42 Koelmans, A.; van der Woude, H.; Hattink, J.; Niesten, D. Long-term bioconcentration kinetics
579 of hydrophobic chemicals in *Selenastrum capricornutum* and *Microcystis aeruginosa*. *Environ.*
580 *Toxicol. Chem.* **1999**, *18*, 1164-1172; DOI 10.1002/etc.5620180614
- 581 43 Swackhamer, D.L.; Skoglund, R.S. Bioaccumulation of PCBs by algae: kinetics versus
582 equilibrium. *Environ. Toxicol. Chem.* **1993**, *12*, 831-838; DOI 10.1002/etc.5620120506
- 583 44 Sobek, A.; Gustafsson, O.; Hajdu, S.; Larsson, U. Particle-water partitioning of PCBs in the
584 photic zone: A 25-month study in the open Baltic Sea. *Environ. Sci. Technol.* **2004**, *38*, 1375-
585 1382; DOI 10.1021/es034447u
- 586 45 Sobek, A.; Cornelissen, G.; Tiselius, P.; Gustafsson, O. Passive partitioning of polychlorinated
587 biphenyls between seawater and zooplankton, a study comparing observed field distributions to
588 equilibrium sorption experiments. *Environ. Sci. Technol.* **2006**, *40*, 6703-6708; DOI
589 10.1021/es061248c
- 590 46 Del Vento, S.; Dachs, J. Prediction of uptake dynamics of persistent organic pollutants by
591 bacteria and phytoplankton. *Environ. Toxicol. Chem.* **2002**, *21*, 2099-2107; DOI
592 10.1002/etc.5620211013
- 593 47 Gobas, F.A.P.C.; Opperhuizen, A.; Hutzinger, O. Bioconcentration of hydrophobic chemicals in
594 fish: relationship with membrane permeation. *Environ. Toxicol. Chem.* **1986**, *5*, 637-646; DOI
595 10.1002/etc.5620050704
- 596 48 Sijm, D.T.H.M.; Van der Linde, A. Size-dependent bioconcentration kinetics of hydrophobic
597 organic chemicals in fish based on diffusive mass transfer and allometric relationships. *Environ.*
598 *Sci. Technol.* **1995**, *29*, 2769-2777; DOI 10.1021/es00011a011

- 599 49 Booij, K.; Tucca, F. Passive samplers of hydrophobic organic chemicals reach equilibrium faster
600 in the laboratory than in the field. *Mar. Pollut. Bull.* **2015**, 98, 365-367; DOI
601 10.1016/j.marpolbul.2015.07.007
- 602 50 Banerjee, S.; Sugatt, R.H.; O'Grady, D.P. A simple method for determining bioconcentration
603 parameters of hydrophobic compounds. *Environ. Sci. Technol.* **1984**, 18, 79-81.
- 604 51 Booij, K.; Vrana, B.; Huckins, J.N.; Greenwood, R.; Mills, G.A.; Vrana, B. Theory, modelling
605 and calibration of passive samplers used in water monitoring, In *Passive sampling techniques in
606 environmental monitoring*; Greenwood, R., Mills, G., Vrana, B., Eds.; Elsevier: Amsterdam,
607 2007; pp. 141-169.
- 608 52 Schäfer, S.; Antoni, C.; Möhlenkamp, C.; Claus, E.; Reifferscheid, G.; Heininger, P.; Mayer, P.
609 Equilibrium sampling of polychlorinated biphenyls in River Elbe sediments – Linking
610 bioaccumulation in fish to sediment contamination. *Chemosphere* **2015**, 138, 856-862; DOI
611 10.1016/j.chemosphere.2015.08.032
- 612 53 Miège, C.; Mazzella, N.; Allan, I.; Dulio, V.; Smedes, F.; Tixier, C.; Vermeirssen, E.; Brant, J.;
613 O'Toole, S.; Budzinski, H.; Ghestem, J.; Staub, P.; Lardy-Fontan, S.; Gonzalez, J.; Coquery, M.;
614 Vrana, B. Position paper on passive sampling techniques for the monitoring of contaminants in
615 the aquatic environment – Achievements to date and perspectives. *Trends Environ. Anal. Chem.*
616 **2015**, 8, 20-26; DOI 10.1016/j.teac.2015.07.001
617